CHAPTER FOURTEEN

# Artificial scaffolds for enhanced biocatalysis

**Qing Sun[a], Shen-Long Tsai[b], Wilfred Chen[c,*]**

[a]Department of Chemical Engineering, Texas A&M University, College Station, TX, United States
[b]Department of Chemical Engineering, National Taiwan University of Science and Technology, Taipei City, Taiwan
[c]Department of Chemical and Biomolecular Engineering, University of Delaware, Newark, DE, United States
*Corresponding author: e-mail address: wilfred@udel.edu

## Contents



## Abstract

Proteins are not designed to be standalone entities and must coordinate their collective action for optimum performance. Nature has developed through evolution the ability to colocalize the functional partners of a cascade enzymatic reaction in order to ensure efficient exchange of intermediates. Inspired by these natural designs, synthetic scaffolds have been created to enhance the overall biological pathway performance. In this chapter, we describe several DNA- and protein-based scaffold approaches to assemble artificial enzyme cascades for a wide range of applications. We highlight the key benefits and drawbacks of these approaches to provide insights on how to choose the appropriate scaffold for different cascade systems.

*Methods in Enzymology*, Volume 617
ISSN 0076-6879
https://doi.org/10.1016/bs.mie.2018.12.007

## 1. Introduction

Many native enzymes are not standalone entities (Fig. 1) but rather organize their collective action within a complex network of proteins (Agapakis, Boyle, & Silver, 2012). The defined function of many cellular processes depends on the exquisite coordination of these enzymes within a highly structured network in order to elicit more complex responses (Quin, Wallin, Zhang, & Schmidt-Dannert, 2017). This controlled organization has been shown to increase the local enzyme and substrate concentrations, enabling improved intermediate channeling between enzymes to avoid competition with other metabolites present in the cell (Lee, DeLoache, & Dueber, 2012).

In nature, many enzymes are frequently clustered together to form a functional metabolon to enhance the efficiency of metabolism via a process called substrate channeling (Menard, Maughan, & Vigoreaux, 2014). By controlling

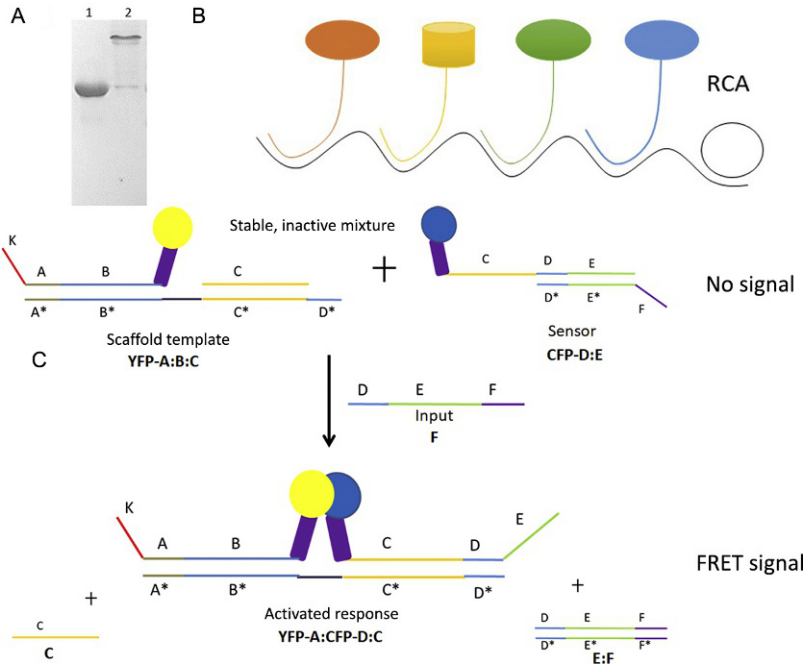


**Fig. 1** Nucleic acid based scaffolding. (A) Conjugation of a DNA oligo onto a halo-tag fusion protein (1). The DNA–protein complex (2) has slower mobility. (B) Enzyme organization on one-dimensional (Sun & Chen, 2016) DNA template with or without rolling circle amplification. (C) Programmed control of protein assembly (Chen et al., 2014). CFP and YFP were brought together onto a single-stranded DNA input.

the spatial and temporal organization of these protein complexes, cellular metabolism can be modulated for optimum efficiency (Jørgensen et al., 2005). In addition to metabolism, interactions between proteins also play a crucial role in defining other cellular functions such as cell signaling, transcription regulation, apoptosis, cellular targeting, and many posttranslational modifications including ubiquitylation (protein degradation) (Blikstad & Ivarsson, 2015; Good, Zalatan, & Lim, 2011). Rather than random clustering, a scaffolding protein is often used to organize multiple binding partners in close proximity to facilitate their concerted interactions and functions (Garbett & Bretscher, 2014).

Inspired by these native examples, artificial scaffolds have been designed to provide defined spatial organization of enzymes for enhanced biocatalysis (Dueber et al., 2009). We have previously demonstrated the use of either DNA-based or protein-based scaffold to assemble synthetic enzyme cascades (Goyal, Tsai, Madan, DaSilva, & Chen, 2011; Liu, Banta, & Chen, 2013; Park, Sun, Liu, DeLisa, & Chen, 2014; Sun & Chen, 2016; Sun, Madan, Tsai, DeLisa, & Chen, 2014; Tsai, DaSilva, & Chen, 2013; Tsai, Goyal, & Chen, 2010; Tsai, Oh, Singh, Chen, & Chen, 2009). We will summarize the benefits and drawbacks of these different strategies for a range of applications.

## 2. Nucleic acid-based scaffolding

The ability to easily predict and manipulate the base-pairing property of nucleic acids along with the ease of synthesis has allowed researchers to create various DNA- or RNA-based nanoscaffolds with one-dimensional, two-dimensional, three-dimensional, and dynamically programmed structures (Pinheiro, Han, Shih, & Yan, 2011). Although enzymes can be chemically functionalized with DNA oligonucleotides to random surface residues, this may lead to activity loss and decrease the universality of this strategy (Fu, Liu, Liu, Woodbury, & Yan, 2012). Even the use of biotinylated enzymes for conjugation to streptavidin-modified DNA oligos is still too labor intensive (Niemeyer, Boldt, Ceyhan, & Blohm, 1999). We have been utilizing a simple genetic approach to generate HaloTag fusion enzymes to enable easy conjugation to chemically modified nucleic acids (Mori et al., 2013).

Our lab reported the generation of four-component artificial cellulosomes onto a DNA scaffold using the self-labeling HaloTag for DNA conjugation. A cellulosome is an organized protein cocktail of three

enzymes, endoglucanase, exoglucanase, and beta-glucosidase, and a carbohydrate binding module (CBM). It is organized through the interaction between the cohesion domains on a surface scaffold and the dockerin domain on the enzymatic subunits. Artificial cellulosomes based on DNA scaffolds have already been achieved in our lab using zinc finger protein (ZFP)-guided assembly (Sun et al., 2014). By fusing CBM and the endoglucanase CelA to two different ZFPs, a two-component cellulosome was created using a double-stranded DNA template with 1.6-fold enhancement in cellulose hydrolysis. Although the enhancement with ZFP-enabled cellulosome assembly was in line with that achieved using protein scaffolds, the major drawback of this strategy is the low binding affinity of ZFPs toward DNA. To improve efficiency and complexity of the artificial cellulosome system, we further conjugated single-stranded DNA onto each protein component to enable cellulosome assembly through DNA hybridization. The self-labeling HaloTag that can form a covalent bond with synthetic chlorohexane (CH)-modified molecules including DNA was used to generate fusions to enable the formation of cellulosome component-DNA complex (Fig. 1A). By combining sequence specific DNA hybridization for four cellulosome components including endoglucanase (CelA from *Clostridium thermocellum*), CBM (from *C. thermocellum*), exoglucanase (CelE from *Clostridium cellulolyticum*), and beta-glucosidase (BglA from *C. thermocellum*), we achieved for the first time full functional artificial cellulosome on DNA template to release glucose from cellulose (Sun & Chen, 2016). Furthermore, by applying longer (>100 repeats) DNA template produced by rolling circle amplification (Fig. 1B), we achieved 5.1-fold enhancement of glucose release compared with free enzymes (Sun & Chen, 2016). To extend the complexity of the protein assembly, we added one additional enzyme glucose oxidase (GOX) to the system by conjugating GOX with a DNA linker via the well-known sulfo-EMCS chemistry (Chen, Yu, Myung, & Chen, 2017). The five-enzyme assembly was able to achieve conversion of cellulose to gluconic acid and $H_2O_2$ with 1.5-fold activity enhancement, suitable for enzyme fuel cell applications.

One specific property of using nucleic acid nanoscaffolds is the feasibility of dynamic assembly by toehold-mediated strand displacement, which involves revealing a new binding sequence in response to the presence of an initiator strand (Zhang & Seelig, 2011). Many such reactions can be linked into a cascade where the newly revealed output sequence of one reaction can initiate another strand displacement reaction elsewhere (Zhang & Seelig, 2011). This, in turn, allows for the construction of chemical reaction networks with many components, exhibiting complex

computational and information processing abilities. Taking advantage of strand displacement, we recently reported the design of multi-input logic circuits programmed control of enzyme assembly (Fig. 1C) (Chen, Blackstock, Sun, & Chen, 2018). This programming system is able to sense DNA or RNA inputs by a predefined signal-processing algorithm to actuate different computational outputs (Han et al., 2012; Linko et al., 2016).

It is clear that nucleic acids can serve as templates for positional immobilization of enzyme cascades both in vivo and in vitro (Delebecque, Lindner, Silver, & Aldaye, 2011; Kim, Sun, Liu, Tsai, & Chen, 2012). Through rational design, both DNA and RNA have been used to create many one-dimensional, two-dimensional, and three-dimensional structures, which are rigid and stable. Furthermore, these structures can program enzyme assemblies through automatic regulation to respond to the environment, the process through the computation logic gate and respond with enzyme activity control, which was achieved through enzyme spatial proximity. All these demonstrated advantages demonstrated further increase the overall activity of enzyme cascades by exploring more favorable arrangements, leading to more favorable substrate channeling.

## 2.1 HaloTag-mediated protein–DNA labeling

To assemble enzymes in a position-specific manner onto a DNA template, we directly conjugated single-stranded DNA oligo onto each protein component to enable enzyme complex assembly through DNA hybridization. Since direct chemical modification of a DNA linker to proteins can sometimes lead to functional loss, the self-labeling HaloTag was used for conjugation. HaloTag is a 34 kDa monomeric mutant haloalkane dehalogenase designed to covalently bind to synthetic CH-modified molecules, including DNA, fluorescent dyes, and solid supports (Sun & Chen, 2016). The covalent attachment is highly specific and occurs rapidly under mild physiological conditions. By genetically tethering HaloTag to the different cellulosomal components, CH-modified DNA oligonucleotides can be site-specifically conjugated for cellulosome assembly (Chen et al., 2017; Sun & Chen, 2016).

### *2.1.1 Equipment*

- Table top centrifuge (Eppendorf)
- Ultrafiltration column (Vivaspin 500, Sartorius Stedim Biotech with 3000 Da cutoff)
- Standard SDS-PAGE equipment, 10% SDS-PAGE gels, 4.5% native acrylamide gel

### 2.1.2 Buffers and reagents

- HaloTag succinimidyl (O4) CH ligand (Promega P6751)
- Oligos with 5′ or 3′ amine modifications

### 2.1.3 Procedure

**A.** The specified oligos with 5′ and 3′ amine modifications were reacted with the HaloTag succinimidyl (O4) CH ligand (Promega P6751) for HaloTag attachment. The CH ligand was mixed with DNA at a molar ratio of 30:1 and incubated at room temperature for 24 h. The excess CH ligand was removed using a 3000 Da ultrafiltration column (Vivaspin 500, Sartorius Stedim Biotech).

**B.** The purified CH-oligos were then reacted with the purified HaloTag fusion protein, using a 3× molar excess of CH-oligo, and incubated overnight at 4°C.

**C.** The excess/unattached oligo was removed by purifying the protein–DNA and washing away any residual DNA through the purifying elastin-like polypeptide (ELP) tag. We added 1 *M* NaCl buffer to the purified protein samples, incubated the sample at 37°C for 10 min and centrifuged for 10 min with 13,000 × *g*. Supernatants were removed and pellets were suspended in cold PBS buffer to get the purified protein–DNA complex.

**D.** The protein only, protein plus excess DNA, and purified protein–DNA samples were loaded onto a 10% SDS-PAGE and stained with Coomassie blue for analysis of labeling efficiency by densitometry.

**E.** The purified protein–DNA samples can then be incubated with single-stranded DNA template with the target sequence for protein immobilization.

**F.** Native PAGE Electromobility shift experiments were carried out in a 4.5% nondenaturing acrylamide gel. The protein only, protein plus DNA linkers, and purified protein–DNA linkers were loaded and run for 45 min at a constant 90 V. The gel was then stained with ethidium bromide for 5 min before imaging.

### 2.1.4 Notes

**A.** Protein fusion with HaloTag was not described, but it is necessary for target protein–DNA labeling.

**B.** Extra molar of CH-oligo can guarantee higher protein–DNA labeling efficiency, which is approximately 100% according to SDS-PAGE gel analysis in our case.

**C.** Elastin-like polypeptide purification is special for our experiments through inverse phase transition (Sun & Chen, 2016; Sun et al., 2014). Other protein purification methods to remove the excess/unattached oligo are also feasible including Myc tag, His-tag, streptavidin tag, and more (Kimple, Brill, & Pasker, 2013).

## 2.2 Zinc finger protein-enabled protein immobilization on DNA template

Nucleic acid binding proteins including ZFPs or RNA aptamer binding domains to organize enzymes has been widely used for both in vitro and in vivo applications. For example, target enzymes can be genetically fused to ZFPs, which have the ability to recognize specific 9–18 base pair sequences of double-stranded DNA. The advantage is that it does not need chemical modification which is time-consuming and might lead to enzyme activity loss. The chemical modification-free process also makes it ideal tools for in vivo enzyme organization on nucleic acid templates. The potential drawback is that these bindings are strongly affinity-dependent and might lead to low organization efficiency (Siu et al., 2015).

### *2.2.1 Equipment*

- Standard native acrylamide gel equipment, 10% native acrylamide gel

### *2.2.2 Buffers and reagents*

- Lightshift Chemiluminescent EMSA kit (Pierce Chemical Co., Rockford, IL)

### *2.2.3 Procedure*

**A.** Purified ZFP fusions were incubated with DNA samples at 37°C for 1 h.

**B.** The complexes were subjected to a 10% native acrylamide gel and run under 90 V for 30 min to check on the binding.

**C.** Membrane transferring and chemiluminescence signaling were conducted with protocols suggested by the manufacturer of the Lightshift Chemiluminescent EMSA kit (Pierce Chemical Co., Rockford, IL).

### *2.2.4 Notes*

**A.** Protein fusion with ZFP was not described, but it is necessary for target protein–DNA template binding.

**B.** The binding affinity of each ZFP is different. To achieve the best usage of this system, the binding affinity of each binding protein should be checked before use.

## 3. Scaffold proteins-based metabolons

Since organisms are limited by the level of protein synthesis, one method to enhance and relax their functionality is by placing functional enzymes in close proximity of each other to control their mutual interaction. Such self-assembled multienzymatic complexes in Nature have long been a source of inspiration for researches to design and construct stable, extensive, and global artificial networks (Chen et al., 2014; Siu et al., 2015). Indeed, several artificial enzyme cascade systems that capitalize on confinement and cooperative effects have been engineered successfully. A basic structure of such elegant machineries includes two parts. First, a scaffold containing multiple affinity domains is used to direct the assembly. Second, enzymes appended with counter-affinity domains to enable their interaction with the scaffold. Recent advances on the creation of artificial metabolon using scaffold portions are depicted in Fig. 2 and details of each format are introduced in the following.

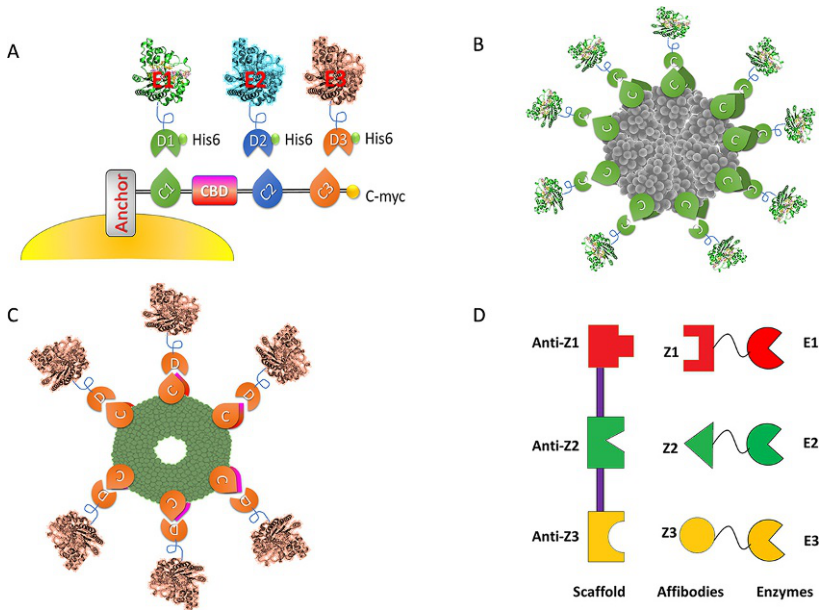


**Fig. 2** Examples of protein-based scaffold: (A) yeast surface displayed mini-cellulosome; (B) assembly of the rosettasome-cohesin scaffold and cellulase chimera; (C) stable protein one (SP1) derived metabolon structure; (D) affibodies as scaffolds for position-specific enzyme assembly.

## 3.1 Cellulosomes

Cellulosomes are one of the most studied extracellular enzyme complexes (Bule, Pires, Fontes, & Alves, 2018). Their fundamental structure consists of catalytic subunits such as cellulases, hemicellulases, pectinases, chitinases, glycosidases, and esterases bound together by noncatalytic scaffold proteins (scaffoldins). The multienzymatic complexes are assembled through the high-affinity interaction between the cohesins of scaffoldins and the dockerins of enzymes. Usually within a given species, the interaction between complementary cohesins and dockerins is nonspecific. This means a dockerin-bearing enzyme can bind to any of the matching cohesins harbored by the scaffoldin with similar affinity (Pinheiro et al., 2012). Via the formation of such a supermolecular structure, the complexed enzymes can hydrolyze cellulose faster than the noncomplexed enzyme mixture due to both substrate-targeting effect and proximity effect.

The first heterologously expressed cellulosomal system was created by Bayer and his coworkers in 1994 (Lamed, Tormo, Chirino, Morag, & Bayer, 1994). Later, by harnessing the species-specific interaction between dockerins and cohesins, artificial cellulosomes of different sizes and architectures have been constructed in vitro to study the functionality of each component in the complex and their impacts on catalytic activities (Adams et al., 2010; Budinova, Mori, Tanaka, & Kamiya, 2018; Fierobe et al., 2002, 2001). For example, several novel cellulosome chimeras exhibiting atypical geometries and binding modes were designed to study its targeting and proximity function (Mingardon, Chanal, Tardif, Bayer, & Fierobe, 2007). Interestingly, in this study diminished activity appeared on the higher-order functional composites, presumably due to the impediment of the mobility of catalytic modules. In contrast, a study investigated the correlation between the sizes of cellulosomal structure to their specific activity and revealed that higher degree of cellulosome complexity resulted in more efficient cellulose hydrolysis with plateaued synergic effects after the cellulosome size reaches certain degree (Chen & Ge, 2018).

Apart from investigating the specific interaction and the synergistic effect of cellulosomal systems in vitro, they also have been displayed on the surface of several microorganisms. The first research that reported the assembly of cellulosomal structure on the cell surface was conducted by the Wilfred Chen's group (Tsai et al., 2009). In this study, the assembly of a minicellulosome on yeast surface was achieved by incubating the lysates of *Escherichia coli* cells that heterologously expressed dockerin-tagged cellulases

with the scaffoldins displayed on yeast surface. Later on, the same group demonstrated the assembly of minicellulosomes can also be accomplished via intracellular complementation in a synthetic yeast consortium (Tsai et al., 2010). Furthermore, an adaptor-scaffoldin-assisted approach was subsequently developed to expand the size of artificial cellulosomal structures on cell surfaces (Tsai et al., 2013). Such cellulosomal structures have also been applied on other microorganisms, such as *E. coli* (Park et al., 2014), *Lactococcus lactis* (Wieczorek & Martin, 2010), *Bacillus subtilis* (Anderson et al., 2011), and *Yarrowia lipolytica* (Yang et al., 2018), for the production of different chemicals from cellulosic biomass.

### 3.1.1 Equipment

- Sonicator
- Bench top centrifuge
- Fluorescence Microscopy
- Ultraviolet–visible spectroscopy
- His-tag purification kits (HisTrap HP 5 mL, GE Healthcare)

### 3.1.2 Buffers and reagents

- Luria-Bertani (LB) medium (10.0 g/L tryptone, 5.0 g/L yeast extract, 10.0 g/L NaCl).
- SGC medium (20.0 g/L galactose, 6.7 g/L yeast nitrogen base w/o amino acids, 5.0 g/L casamino acids).
- SDC medium (20.0 g/L dextrose, 6.7 g/L yeast nitrogen base w/o amino acids, 5.0 g/L casamino acids).
- Antibiotic stock solution (100 mg/mL ampicillin or 50 mg/mL kanamycin).
- Tris–HCl, pH 8.0, 100 m*M* NaCl, and 10 m*M* $CaCl_2$.
- Anti-C-Myc or anti-C-His antibody from mouse.
- Anti-mouse IgG conjugated with Alexa 488.

### 3.1.3 Procedures

1. Yeast cells (*Saccharomyces cerevisiae* EBY100 in this case) were precultured in an SDC medium for 18 h with shaking at 30°C.
2. These precultures were then subinoculated into an SGC medium with an optical density (OD) at 600 nm of 0.1.
3. Growth for 48 h with shaking at 20°C for the induction of yeast displayed scaffoldins.

4. *E. coli* strains (BL21 (DE3) in this case) overexpressing dockerin-tagged cellulases were precultured in test tubes at 37°C in LB medium supplemented with appropriate antibiotics overnight.
5. Overnight cultures were regrown in a new LB medium supplemented with 1.5% glycerol and appropriate antibiotics with an initial OD of 0.01 at 37°C until OD reached 1.5.
6. The cultures were then cooled to 20°C, and isopropyl thio-β-D-galactoside (IPTG) was added to a final concentration of 200 μ*M*.
7. After 16 h the cells were harvested by centrifugation (3000 × *g*, 10 min) at 4°C, resuspended in 50 m*M* Tris–HCl and broken in ice by a sonicator.
8. Cellulases in *E. coli* cell lysates were purified with a His-tag purification kits (HisTrap HP 5 mL, GE Healthcare) at 4°C. Buffers used were following the protocol provided by the vender.
9. Incubating the dockerin-tagged cellulases with the yeast cells that displaying scaffoldins on the surface for 1 h at 4°C in 50 m*M* Tris–HCl.
10. The yeast cells were washed and harvested by centrifugation (3000 × *g*, 10 min) at 4°C, and then resuspended in the same buffer for further Microscopy.
11. The cells were resuspended in 250 μL of PBS buffer containing 1 mg/mL BSA, and 0.5 μg of anti-C-Myc or anti-C-His for 4 h with occasional mixing.
12. Cells were then pelleted and washed with Tris–HCl before resuspending in Tris–HCl buffer plus 1 mg/mL BSA and 0.5 μg anti-mouse IgG conjugated with Alexa 488.
13. After incubated for 2 h, cells were pelleted and wished twice with PBS, followed by resuspension in PBS buffer to an OD around 1.
14. 5–10 μL of cell suspensions were spotted on slides and added coversilps for fluorescence microscopy. The excitation wavelength was 485 nm and the emission wavelength was 535 nm.

### *3.1.4 Notes*

1. The procedure described here is for the assembly of minicellulosomes on the yeast surface. It can be adapted accordingly to other microorganisms as well.
2. Cellulases on the dockerin-tagged catalytic subunits can be replaced by other enzymes based on the requirement of reactions.
3. Dockerin/cohesin pairs from other species with their own specificity can also be applied to extend the positional-specific supramolecular structure.

## 3.2 Rosettasome

Inspired by the mechanisms of cellulosome assembly and the improved catalytic activity, the high-affinity interaction between dockerin and cohesin has been adapted and fused to other proteins to create several cellulosome-mimic structures. Mitsuzawa and coworkers created a synthetic cellulosome containing 4 different cellulases assembled on an 18-subunit protein complex called a rosettasome (Mitsuzawa et al., 2009). Rosettasome is originally a group II chaperonin that self-assembles into double rings in the presence of ATP and magnesium ions. When all four enzymes were present in the complex, enhanced cellulase activity was observed when compared to the free enzymes or the unassembled rosettasome. Recently, three different enzymes involved in both biomass hydrolysis and oxidative transformation to glucaric acid were tethered onto a rosettasome scaffold. A 40% higher production enhancement in a combined hydrolysis and bioconversion metabolic pathway was also obverted analogously as compared to the uncomplexed enzymes (Lee, Kibblewhite, Paavola, Orts, & Wagschal, 2016).

### 3.2.1 Equipment

- Sonicator
- Bench top centrifuge
- Ultraviolet–visible spectroscopy
- His-tag purification kits (GE Healthcare)
- Ultrafiltration column (25 kDa cutoff)
- DEAE and MonoQ columns (GE Healthcare, formerly Amersham Biosciences)
- Centriprep YM30 centrifugal concentrators (Millipore)

### 3.2.2 Buffers and reagents

- Elution buffer (25 m*M* HEPES, 1 m*M* EDTA pH 7.5, 1–400 m*M* NaCl).
- 20 m*M* Tris–HCl (pH 8.0).
- Rosettasome–cohesin assembly buffer (1 m*M* ATP and 25 m*M* $Mg^{2+}$)
- Rosettazymes assembly buffer (50 m*M* Tris–maleate buffer (pH 6.0) containing 0.7 m*M* ATP, 17.4 m*M* $MgCl_2$, and 5 m*M* $CaCl_2$)

### 3.2.3 Procedures

1. Procedures for the expression of recombinant proteins were similar as described previously (see Section 3.1.3).
2. The cell lysate was centrifuged (17,000 × *g*, 4°C, 30 min) after sonication and, if required, a heat precipitation was performed at 65°C.

3. The nucleic acids were precipitated by adding 1% (v/v) of a 10% (w/v) polyethyleneimine stock solution, pH 7.8.
4. The rosettasome–cohesin protein was purified chromatographically using DEAE (a weak anion exchange chromatography column) and MonoQ (a strong anion exchange chromatography column) columns at a 1–400 m*M* NaCl elution gradient in 25 m*M* HEPES, 1 m*M* EDTA pH 7.5.
5. Between columns, fractions were pooled and dialyzed overnight using a 25,000 MWCO SpectraPor 7 cellulose dialysis membrane in 25 m*M* HEPES, 0.1 m*M* EDTA pH 7.5 buffer at room temperature.
6. The fractionated protein was concentrated using Centriprep YM30 centrifugal concentrators. Buffer was exchanged using an ultrafiltration column and 20 m*M* Tris–HCl (pH 8.0).
7. Rosettasome–cohesin double rings were assembled by mixing subunits (2 mg/mL) with ATP/$Mg^{2+}$ (1 m*M*/25 m*M*) and incubating at 4°C overnight.
8. Rosettazymes or cellulase mixtures were formed by mixing 7.72 μ*M* rosettasome–cohesin double rings or ATP/$Mg^{2+}$ (1 m*M*/25 m*M*) with 6.86 μ*M* cellulases and incubating at room temperature for >5 min in rosettazymes assembly buffer.

#### 3.2.4 Notes

1. Some fusion proteins may be purified from inclusion bodies. In this case, the protein pellet may be dissolved in 5 *M* urea, 0.1 *M* Tris (pH 8.0) for 60 min at room temperature and then refolded overnight in 20 m*M* Tris–HCl, 1.5 m*M* cellobiose, 0.1 m*M* EDTA (pH 8.0) with stirring.
2. Cellulases on the dockerin-tagged catalytic subunits can be replaced by other enzymes based on the requirement of reactions.
3. The interaction between dockerin and cohesion is calcium-dependent. The presence of calcium is necessary for the assembly.

### 3.3 Stress-responsive protein

The stable protein one (SP1) isolated from *Populus tremula* is a thermal stable and stress-responsive protein. It is a ring-like protein that consists of 12 subunits tightly bound to each other via hydrophobic interactions (Dgany et al., 2004). SP1 is an even better candidate of scaffold proteins due to its special features, such as the high stability at high-temperature, the broad pH tolerances, and the resistance to organic solvents. Taking advantages of its self-assembly characteristic, GOX has been fused in-frame to SP1 to

create multienzyme nanotubes containing hundreds of active enzyme molecules per tube (Heyman, Levy, Altman, & Shoseyov, 2007). As a mimic to cellulosomal structure, SP1 scaffold also has been fused with cohesin modules to which dockerin-bearing exogluconases were linked. A more than fourfold increase in the hydrolytic activity of cellulosic substrates was achieved by the complexed cellulases as compared to that by the uncomplexed cellulases (Morais et al., 2010).

### 3.3.1 Equipment

- Sonicator
- Bench top centrifuge
- Ultraviolet–visible spectroscopy
- His-tag purification kits (GE Healthcare)
- Ultrafiltration column (5 kDa cutoff)

### 3.3.2 Buffers and reagents

- TBS buffer (136 m*M* NaCl, 2.5 m*M* KCl, 25 m*M*, pH 7.4)
- Protease inhibitor product no. 1836145 (Roche Diagnostics, Mannheim, Germany)
- Tris-buffered saline (137 m*M* NaCl, 2.7 m*M* KCl, 25 m*M* Tris–HCl, pH 7.4)
- 4.5% native acrylamide gel

### 3.3.3 Procedures

1. Procedures for the expression of recombinant proteins were similar as described previously (see Section 3.1.3).
2. *E. coli* BL21 (DE3) bacteria expressing Coh-SP1 were lysed by sonication on ice for several minutes with pulsed bursts in TBS buffer plus complete protease inhibitor.
3. Soluble proteins were separated by centrifugation at $13{,}000 \times g$ for 10 min and purified by His-tag purification kits.
4. *E. coli* BL21 bacteria expressing cellulase chimera were lysed by sonication on ice for several minutes with pulsed bursts in Tris-buffered saline supplemented with 2 m*M* $CaCl_2$.
5. The crude protein extract containing Cel5A was added to a 15 mL aqueous (pH 7.3) suspension of 7.5 g/L phosphoric acid-swollen cellulose (PASC) and stirred for 1 h.
6. After centrifugation, the pellet was washed three times with TBS containing 1 *M* NaCl, and three times with TBS alone.

7. The CBM-containing proteins were eluted using 12 mL of 1% (v/v) trimethylamine and then neutralized with 1 *M* 2-(*N*-morpholino) ethanesulfonic acid.
8. Protein samples were concentrated by centrifugation (3000 × *g*, 2 h), using 5000 Da cutoff ultrafiltration column.
9. Coh-SP1 and cellulase chimera were mixed at a molar ratio of 1:18, respectively, in TBS buffer containing 10 m*M* $CaCl_2$, 0.05% Tween 20 and incubated for 1 h at 37°C.
10. The assembled complexes were analyzed by 4.5% native acrylamide gel.

#### 3.3.4 Notes

1. In some cases, BL21 pLysS may be used for the expression of cellulase chimera.
2. Remember to use 1% $NaHCO_3$ to neutralize the PASC after its preparation.
3. Cellulases on the dockerin-tagged catalytic subunits can be replaced by other enzymes based on the requirement of reactions.
4. The interaction between dockerin and cohesion is calcium-dependent. The presence of calcium is necessary for the assembly.

### 3.4 Affibody

Affibody binding proteins are functionally selected from libraries of a small (6 kDa) and noncysteine three-helix bundle domains (Lofblom et al., 2010). Due to their structurally less complex as compared to immunoglobulins, they are expected to offer advantages as scaffold proteins. Indeed affibodies have been used to drive colocalization of affibody-labeling enzymes in a cascaded metabolic channel. By coexpression of an affibody-based synthetic scaffold that provides an anchor site for two or three counter-tagged enzymes expressed in the same cell, it was found that the yield of farnesene is increased by 135% in *S. cerevisiae*. Similarly, in *E. coli*, the yield of poly-hydroxybutyrate increased by 700% compared to the control (Tippmann et al., 2017).

#### 3.4.1 Equipment

- Ultraviolet–visible spectroscopy
- High-performance liquid chromatography (HPLC)

### 3.4.2 Buffers and reagents

- YPD plates (20 g/L glucose, 10 g/L yeast extract, 20 g/L peptone from casein, and 20 g/L agar).
- Selective growth medium (6.9 g/L yeast nitrogen base w/o amino acids, 0.77 g/L complete supplement mixture, 20 g/L glucose, and 20 g/L agar).
- Minimal medium (30 g/L glucose, 7.5 g/L $(NH_4)_2SO_4$, 14.4 g/L $KH_2PO_4$, 0.5 g/L $MgSO_4{\cdot}7H_2O$, and 1 mL/L trace element solution).
- LB medium (10.0 g/L tryptone, 5.0 g/L yeast extract, and 10.0 g/L NaCl)

### 3.4.3 Procedures

1. Strains of *S. cerevisiae* were grown and maintained on plates with selective medium at 30°C.
2. 5 mL of minimal medium containing 30 g/L glucose were inoculated with a single colony and cultivated overnight at 30°C and 200 rpm.
3. The culture was used to inoculate 18 mL of minimal medium to an $OD_{600}$ of 0.1.
4. To sequester farnesene, 2 mL of dodecane was added to reach a final concentration of 10% (v/v).
5. Shake flasks were cultivated at 180 rpm and 30°C for 72 h.
6. Farnesene concentration was analyzed with HPLC appended with diode array detection.

### 3.4.4 Notes

1. Affibodies can be functionally selected from libraries of a small (6 kDa), noncysteine three-helix bundle domain used as a scaffold. The libraries have typically been displayed on phages, followed by biopanning against desired targets.

## 3.5 Other affinity proteins as scaffolds

Inspired by the assembly mechanisms of cellulosomes in nature, synthetic metabolons that used different affinity tags to replace dockerins on the scaffoldin and dockerins on the catalytic enzymes, or different enzymes to replace cellulases in the cellulosomes were developed. For example, rather than using dockerins and cohesins, one protein pair consists of the Z domain of protein A derived from *Staphylococcus aureus* and the Fc domain of human immunoglobulin G was used to construct a novel cellulosomal system that could control the ratio of target proteins on the surface of *S. cerevisiae*.

In 2009, Dueber et al. colocalized three mevalonate biosynthesis enzymes (AtoB, HMGS, and HMGR) in vivo by engineering an artificial

scaffold which contained three different protein–protein interaction domains (PDZ, GBD, and SH3). By modulating the ratio of these domains, optimization of the stoichiometry among the three mevalonate biosynthetic enzymes recruited to the synthetic complex could be achieved. A 77-fold increase in product titer was obtained compared to the nonscaffolded pathway. The stoichiometry of repeats and the order of interaction domains were varied to control the pathway flux, indicating that the increase in product titer was not just a result of coimmobilization. Interestingly, in another study that used the same domains to increase the production of glucaric acid in *E. coli* showed only a limited pathway-enhancing effect. The production titer of glucaric acid was improved by only fivefold compared to the control group (Moon, Dueber, Shiue, & Prather, 2010). It seems like that enzymatic diversity within the scaffold is crucial for the significance of the activity improvement.

Swapping only the catalytic domain in the cellulosomal structure for activity enhancement toward other cascade reactions can also be accomplished. Liu et al. created a multienzyme metabolon for completing methanol cascade oxidation (Liu et al., 2013). In this study, docking the three required dehydrogenases (alcohol dehydrogenase, formaldehyde dehydrogenase, and formate dehydrogenase) onto a trifunctional synthetic scaffold displayed on the yeast surface was achieved via the high-affinity interaction between dockerins and cohesins. The position-specific and sequential assembly of three dehydrogenases on the displayed scaffold facilitates the efficient substrate channeling, resulting in more than five times higher NADH production rate than that of the noncomplexed enzymes. Another interesting example for demonstrating this concept was conducted by Hyeon and his colleagues for biological conversion of carbon monoxide to carbon dioxide (Hyeon, Kim, Park, & Han, 2015). A carbon monoxide dehydrogenase and a carbon monoxide-binding protein were applied as a catalytic enzyme and enhanced substrate for binding, respectively, to construct a CO-conversion-complexed system with enhanced efficiency. To assemble the complexed system, both CO-related enzymes were fused with dockerin module and bound to the scaffolding protein mCbpA containing two cohesin modules. The scaffolding protein was anchored on the cell surface of the $CO_2$-utilizing *Ralstonia eutropha*. The designed cell-surface-displayed CO-conversion system successfully increased the conversion efficiency of CO through both the substrate-binding-affinity effect and the enzyme proximity effect. This example successfully demonstrated that cellulosomal structures could easily be modified to fit different needs in metabolic engineering or synthetic biology researches to produce more valuable products.

## 4. Summary and conclusion

Scaffold proteins play important roles in a variety of biological processes, from simple mechanisms such as binding and stratification to control the specificity and dynamics of metabolism transfer to more complex behaviors such as precisely controlled signaling cascades. Inspired by such elegant suprabiomolecular interactions, synthetic biomolecular scaffolds are used to construct new and predictable signals or metabolic networks to program useful cellular behavior in the laboratory. The versatility of scaffold biomolecules comes from their modularity and benefits gained through synthetic scaffolds have become a complementary and parallel approach to provide additional control over biocatalysis fluxes by altering local enzyme stoichiometry and exerting spatial and ratio control over enzyme clustering. Both nucleic acids and proteins can serve as templates for positional immobilization of enzyme cascades to enhance biocatalysis efficiency both in vivo and in vitro. ZFP-enabled enzyme immobilization provides advantages for both in vivo and in vitro usage but may suffer from low binding affinity if not well designed. HaloTag provides another possibility of covalent enzyme–DNA complex formation and thus is good for in vitro applications. Via the specific interaction between dockerins and cohesins, cellulosome structures have been applied on the surface of different microorganisms and multimeric proteins to create suprabiomolecules that process improved specificity. Obviously, by precisely harnessing the specificity and modularity of biomolecules, one-dimensional, two-dimensional, and three-dimensional supramolecular structures could be created through rational design to pave ways for organizing enzymes that can enhance product yields or respond to environmental stimuli.

## References

Adams, J. J., Currie, M. A., Ali, S., Bayer, E. A., Jia, Z. C., & Smith, S. P. (2010). Insights into higher-order organization of the cellulosome revealed by a dissect-and-build approach: Crystal structure of interacting *Clostridium thermocellum* multimodular components. *Journal of Molecular Biology*, *396*(4), 833–839.

Agapakis, C. M., Boyle, P. M., & Silver, P. A. (2012). Natural strategies for the spatial optimization of metabolism in synthetic biology. *Nature Chemical Biology*, *8*(6), 527–535.

Anderson, T. D., Robson, S. A., Jiang, X. W., Malmirchegini, G. R., Fierobe, H. P., Lazazzera, B. A., et al. (2011). Assembly of minicellulosomes on the surface of *Bacillus subtilis*. [Retracted article. See vol. 84, unsp. e02429-17, 2018]. *Applied and Environmental Microbiology*, *77*(14), 4849–4858.

Blikstad, C., & Ivarsson, Y. (2015). High-throughput methods for identification of protein-protein interactions involving short linear motifs. *Cell Communication and Signaling: CCS*, *13*(1), 38. https://doi.org/10.1186/s12964-015-0116-8.

Budinova, G. A. L. G., Mori, Y., Tanaka, T., & Kamiya, N. (2018). Casein-based scaffold for artificial cellulosome design. *Process Biochemistry*, *66*, 140–145.

Bule, P., Pires, V. M. R., Fontes, C. M. G. A., & Alves, V. D. (2018). Cellulosome assembly: Paradigms are meant to be broken! *Current Opinion in Structural Biology*, *49*, 154–161.

Chen, R. P., Blackstock, D., Sun, Q., & Chen, W. (2018). Dynamic protein assembly by programmable DNA strand displacement. *Nature Chemistry*, *10*(4), 474–481. https://doi.org/10.1038/s41557-018-0016-9.

Chen, R., Chen, Q., Kim, H., Siu, K. H., Sun, Q., Tsai, S. L., et al. (2014). Biomolecular scaffolds for enhanced signaling and catalytic efficiency. *Current Opinion in Biotechnology*, *28*, 59–68. https://doi.org/10.1016/j.copbio.2013.11.007.

Chen, L., & Ge, X. (2018). Correlation between size and activity enhancement of recombinantly assembled cellulosomes. *Applied Biochemistry and Biotechnology*, *186*, 1–12.

Chen, Q., Yu, S., Myung, N., & Chen, W. (2017). DNA-guided assembly of a five-component enzyme cascade for enhanced conversion of cellulose to gluconic acid and H2O2. *Journal of Biotechnology*, *263*, 30–35. https://doi.org/10.1016/j.jbiotec.2017.10.006.

Delebecque, C. J., Lindner, A. B., Silver, P. A., & Aldaye, F. A. (2011). Organization of intracellular reactions with rationally designed RNA assemblies. *Science*, *333*(6041), 470–474. https://doi.org/10.1126/science.1206938.

Dgany, O., Gonzalez, A., Sofer, O., Wang, W. X., Zolotnitsky, G., Wolf, A., et al. (2004). The structural basis of the thermostability of SP1, a novel plant (*Populus tremula*) boiling stable protein. *Journal of Biological Chemistry*, *279*(49), 51516–51523.

Dueber, J. E., Wu, G. C., Malmirchegini, G. R., Moon, T. S., Petzold, C. J., Ullal, A. V., et al. (2009). Synthetic protein scaffolds provide modular control over metabolic flux. *Nature Biotechnology*, *27*, 753–759. https://doi.org/10.1038/nbt.1557.

Fierobe, H. P., Bayer, E. A., Tardif, C., Czjzek, M., Mechaly, A., Belaich, A., et al. (2002). Degradation of cellulose substrates by cellulosome chimeras—Substrate targeting versus proximity of enzyme components. *Journal of Biological Chemistry*, *277*(51), 49621–49630.

Fierobe, H. P., Mechaly, A., Tardif, C., Belaich, A., Lamed, R., Shoham, Y., et al. (2001). Design and production of active cellulosome chimeras—Selective incorporation of dockerin-containing enzymes into defined functional complexes. *Journal of Biological Chemistry*, *276*(24), 21257–21261.

Fu, J., Liu, M., Liu, Y., Woodbury, N. W., & Yan, H. (2012). Interenzyme substrate diffusion for an enzyme cascade organized on spatially addressable DNA nanostructures. *Journal of the American Chemical Society*, *22*, 13–16.

Garbett, D., & Bretscher, A. (2014). The surprising dynamics of scaffolding proteins. *Molecular Biology of the Cell*, *25*(16), 2315–2319. https://doi.org/10.1091/mbc.E14-04-0878.

Good, M. C., Zalatan, J. G., & Lim, W. A. (2011). Scaffold proteins: Hubs for controlling the flow of cellular information. *Science*, *332*(6030), 680–686. https://doi.org/10.1126/science.1198701.

Goyal, G., Tsai, S. L., Madan, B., DaSilva, N. A., & Chen, W. (2011). Simultaneous cell growth and ethanol production from cellulose by an engineered yeast consortium displaying a functional mini-cellulosome. *Microbial Cell Factories*, *10*, 8. https://doi.org/10.1186/1475-2859-10-89.

Han, D., Zhu, Z., Wu, C., Peng, L., Zhou, L., Gulbakan, B., et al. (2012). A logical molecular circuit for programmable and autonomous regulation of protein activity using DNA aptamer-protein interactions. *Journal of the American Chemical Society*, *134*(51), 20797–20804. https://doi.org/10.1021/ja310428s.

Heyman, A., Levy, I., Altman, A., & Shoseyov, O. (2007). SP1 as a novel scaffold building block for self-assembly nanofabrication of submicron enzymatic structures. *Nano Letters*, *7*(6), 1575–1579.

Hyeon, J. E., Kim, S. W., Park, C., & Han, S. O. (2015). Efficient biological conversion of carbon monoxide (CO) to carbon dioxide (CO2) and for utilization in bioplastic

production by Ralstonia eutropha through the display of an enzyme complex on the cell surface. *Chemical Communications*, *51*(50), 10202–10205.

Jørgensen, K., Rasmussen, A. V., Morant, M., Nielsen, A. H., Bjarnholt, N., Zagrobelny, M., et al. (2005). Metabolon formation and metabolic channeling in the biosynthesis of plant natural products. *Current Opinion in Plant Biology*, *8*(3), 280–291. https://doi.org/10.1016/j.pbi.2005.03.014.

Kim, H., Sun, Q., Liu, F., Tsai, S. L., & Chen, W. (2012). Biologically assembled nanobiocatalysts. *Topics in Catalysis*, *55*(16–18), 1138–1145. https://doi.org/10.1007/s11244-012-9897-9.

Kimple, M. E., Brill, A. L., & Pasker, R. L. (2013). Overview of affinity tags for protein purification. *Current Protocol in Protein Science, 73,* Unit 9.9, 9.9.1-9.9.23, https://doi.org/10.1002/0471140864.ps0909s73.

Lamed, R., Tormo, J., Chirino, A. J., Morag, E., & Bayer, E. A. (1994). Crystallization and preliminary-X-ray analysis of the major cellulose-binding domain of the cellulosome from *Clostridium-thermocellum*. *Journal of Molecular Biology*, *244*(2), 236–237.

Lee, H., DeLoache, W. C., & Dueber, J. E. (2012). Spatial organization of enzymes for metabolic engineering. *Metabolic Engineering*, *14*(3), 242–251. https://doi.org/10.1016/j.ymben.2011.09.003.

Lee, C. C., Kibblewhite, R. E., Paavola, C. D., Orts, W. J., & Wagschal, K. (2016). Production of glucaric acid from hemicellulose substrate by rosettasome enzyme assemblies. *Molecular Biotechnology*, *58*(7), 489–496.

Linko, V., Nummelin, S., Aarnos, L., Tapio, K., Toppari, J., & Kostiainen, M. (2016). DNA-based enzyme reactors and systems. *Nanomaterials*, *6*(8), 139. https://doi.org/10.3390/nano6080139.

Liu, F., Banta, S., & Chen, W. (2013). Functional assembly of a multi-enzyme methanol oxidation cascade on a surface-displayed trifunctional scaffold for enhanced NADH production. *Chemical Communications*, *49*(36), 3766–3768. https://doi.org/10.1039/c3cc40454d.

Lofblom, J., Feldwisch, J., Tolmachev, V., Carlsson, J., Stahl, S., & Frejd, F. Y. (2010). Affibody molecules: Engineered proteins for therapeutic, diagnostic and biotechnological applications. *FEBS Letters*, *584*(12), 2670–2680.

Menard, L., Maughan, D., & Vigoreaux, J. (2014). The structural and functional coordination of glycolytic enzymes in muscle: Evidence of a metabolon? *Biology*, *3*(3), 623–644.

Mingardon, F., Chanal, A., Tardif, C., Bayer, E. A., & Fierobe, H. P. (2007). Exploration of new geometries in cellulosome-like chimeras. *Applied and Environmental Microbiology*, *73*(22), 7138–7149.

Mitsuzawa, S., Kagawa, H., Li, Y. F., Chan, S. L., Paavola, C. D., & Trent, J. D. (2009). The rosettazyme: A synthetic cellulosome. *Journal of Biotechnology*, *143*(2), 139–144.

Moon, T. S., Dueber, J. E., Shiue, E., & Prather, K. L. (2010). Use of modular, synthetic scaffolds for improved production of glucaric acid in engineered E. coli. *Metabolic Engineering*, *12*, 298–305.

Morais, S., Heyman, A., Barak, Y., Caspi, J., Wilson, D. B., Lamed, R., et al. (2010). Enhanced cellulose degradation by nano-complexed enzymes: Synergism between a scaffold-linked exoglucanase and a free endoglucanase. *Journal of Biotechnology*, *147*(3–4), 205–211.

Mori, Y., Ozasa, S., Kitaoka, M., Noda, S., Tanaka, T., Ichinose, H., et al. (2013). Aligning an endoglucanase Cel5A from Thermobifida fusca on a DNA scaffold: potent design of an artificial cellulosome. *Chemical Communications (Cambridge, England)*, *49*(62), 6971–6973. https://doi.org/10.1039/c3cc42614a.

Niemeyer, C. M., Boldt, L., Ceyhan, B., & Blohm, D. (1999). DNA-directed immobilization: Efficient, reversible, and site-selective surface binding of proteins by means of covalent DNA-streptavidin conjugates. *Analytical Biochemistry*, *268*(1), 54–63. https://doi.org/10.1006/abio.1998.3017.

Park, M., Sun, Q., Liu, F., DeLisa, M. P., & Chen, W. (2014). Positional assembly of enzymes on bacterial outer membrane vesicles for cascade reactions. *PLoS One*, *9*(5), e97103. https://doi.org/10.1371/journal.pone.0097103.

Pinheiro, B. A., Bras, J. L. A., Najmudin, S., Carvalho, A. L., Ferreira, L. M. A., Prates, J. A. M., et al. (2012). Flexibility and specificity of the cohesin-dockerin interaction: Implications for cellulosome assembly and functionality. *Biocatalysis and Biotransformation*, *30*(3), 309–315.

Pinheiro, A. V., Han, D., Shih, W. M., & Yan, H. (2011). Challenges and opportunities for structural DNA nanotechnology. *Nature Nanotechnology*, *6*(12), 763–772. https://doi.org/10.1038/nnano.2011.187.

Quin, M. B., Wallin, K. K., Zhang, G., & Schmidt-Dannert, C. (2017). Spatial organization of multi-enzyme biocatalytic cascades. *Organic & Biomolecular Chemistry*, *15*(20), 4260–4271. https://doi.org/10.1039/C7OB00391A.

Siu, K. H., Chen, R. P., Sun, Q., Chen, L., Tsai, S. L., & Chen, W. (2015). Synthetic scaffolds for pathway enhancement. *Current Opinion in Biotechnology*, *36*, 98–106. https://doi.org/10.1016/j.copbio.2015.08.009.

Sun, Q., & Chen, W. (2016). HaloTag mediated artificial cellulosome assembly on a rolling circle amplification DNA template for efficient cellulose hydrolysis. *Chemical Communications*, *52*(40), 6701–6704. https://doi.org/10.1039/c6cc02035f.

Sun, Q., Madan, B., Tsai, S.-L., DeLisa, M. P., & Chen, W. (2014). Creation of artificial cellulosomes on DNA scaffolds by zinc finger protein-guided assembly for efficient cellulose hydrolysis. *Chemical Communications (Cambridge, England)*, *50*(12), 1423–1425. https://doi.org/10.1039/c3cc47215a.

Tippmann, S., Anfelt, J., David, F., Rand, J. M., Siewers, V., Uhlen, M., et al. (2017). Affibody scaffolds improve sesquiterpene production in *Saccharomyces cerevisiae*. *ACS Synthetic Biology*, *6*(1), 19–28.

Tsai, S. L., DaSilva, N. A., & Chen, W. (2013). Functional display of complex cellulosomes on the yeast surface via adaptive assembly. *ACS Synthetic Biology*, *2*(1), 14–21. https://doi.org/10.1021/sb300047u.

Tsai, S. L., Goyal, G., & Chen, W. (2010). Surface display of a functional minicellulosome by intracellular complementation using a synthetic yeast consortium and its application to cellulose hydrolysis and ethanol production. *Applied and Environmental Microbiology*, *76*(22), 7514–7520. https://doi.org/10.1128/aem.01777-10.

Tsai, S. L., Oh, J., Singh, S., Chen, R. Z., & Chen, W. (2009). Functional assembly of minicellulosomes on the *Saccharomyces cerevisiae* cell surface for cellulose hydrolysis and ethanol production. *Applied and Environmental Microbiology*, *75*(19), 6087–6093. https://doi.org/10.1128/aem.01538-09.

Wieczorek, A. S., & Martin, V. J. J. (2010). Engineering the cell surface display of cohesins for assembly of cellulosome-inspired enzyme complexes on *Lactococcus lactis*. *Microbial Cell Factories*, *9*, 69.

Yang, K., Li, F., Qiao, Y., Zhou, Q., Hu, Z., He, Y., et al. (2018). Design of a new multienzyme complex synthesis system based on *Yarrowia lipolytica* simultaneously secreted and surface displayed fusion proteins for sustainable production of fatty acid-derived hydrocarbons. *ACS Sustainable Chemistry & Engineering*, *6*, 17035–17043.

Zhang, D. Y., & Seelig, G. (2011). Dynamic DNA nanotechnology using strand-displacement reactions. *Nature Chemistry*, *3*(2), 103–113. https://doi.org/10.1038/nchem.957.

This page intentionally left blank